Defence Science Journal, Vol. 73, No. 4, July 2023, pp. 437-444, DOI : 10.14429/dsj.73.17885

Compact UWB Monopole Antenna With Tunable Dual Band Notched Characteristics for WiMAX and WLAN Applications

Vikas Kumar Rai* and Mithilesh Kumar

Department of Electronics Engineering, Rajasthan Technical University, Kota - 324 010, India
**E-mail: hellovikasrai@yahoo.com*

ABSTRACT

The present work shows a planar compact ultra-wideband (UWB) monopole antenna with controllable dual band-notch frequencies at 3.3 GHz for WiMAX and 5 GHz for WLAN. In the proposed antenna, the lower notch band (at a frequency of 3.3 GHz) is made by cutting a thin horizontal strip on top of the radiating patch. The upper notch band (at a frequency of 5 GHz) is made by putting two narrow parasitic strips in the shape of an "I" on either side of the radiating patch. The incorporation of three varactor diodes between the radiating patch and three metallic strips provides the flexibility of adjusting the notch frequencies. The notch band tunability between 3.15 GHz and 3.69 GHz and between 4.93 GHz and 5.59 GHz, respectively, is achieved by changing the bias voltage of the varactor diode between 0 V and 30 V. The gain and efficiency characteristics of the designed antenna also exhibit band rejection at the respective notch frequencies. The design principle is validated by fabricating and measuring a prototype of the proposed dual-band, notched UWB antenna. For three different bias voltages of the varactor, the simulated and experimental findings are in reasonable agreement. The proposed works demonstrate better-notch characteristics as compared with other reported works over the UWB range.

Keywords: Ultra-wideband; Dual-band; Tunable; Monopole antenna

1. INTRODUCTION

The FCC (Federal Communication Commission) allocated the Ultra-Wideband (UWB) communication spectrum (3.1–10.6 GHz) to unlicensed users in 2002 because there wasn't much spectrum left to add new services while keeping existing ones[1-2]. UWB technology is one of the most widely used types of wireless communication today. This is because it has a short range, a high data rate, and uses little energy. The development of UWB monopole antennas is also very important for the UWB communication system because it is hard to get impedance matching over a wide frequency range. So, many researchers have come up with different antenna structures that could fulfill this wide-band function. Existing narrow bands for other communication systems, like WiMAX, WLAN, etc., may interfere with the allowed UWB frequency band[3-4]. Band-notch UWB antennas are good for getting around this interference problem.

Further, many strategies have been documented in the literature[5–12] for producing notch characteristics with UWB antennas. Etching slots into the radiating surface and/or ground plane is a common technique[5-8]. Other techniques include placing a parasitic element(s) next to the radiating element, as well as other ways[9-12]. Usually, one slot or parasitic strip is sufficient to generate a single notch. However, to generate a dual-notch, it requires either two different slots or two parasitic elements with different lengths. Further, the notch frequency, generated using slots or parasitic elements, cannot be adjusted after fabrication. It is also necessary for some applications to adjust the notch frequency as per the requirements. Thus, to get the tunable or reconfigurable notched behavior, several switching devices, like MEMS (Micro Electro Mechanical Switch), PIN diodes, and varactor diodes, have been incorporated in UWB band-notched antennas. The notch frequency of the UWB antenna is mostly realised for a single or dual band in[13-27].

This paper proposes a simple UWB monopole antenna with two notch bands and independent notch frequency control. It is possible to change the capacitance of the varactor diode to eliminate interference between the frequencies used by WiMAX and WLAN. The capacitance of a varactor diode can be changed by altering the bias voltage. The developed antenna can operate between 2 and 14 GHz. By adjusting the capacitance of the varactor diode on the strip in a manner that is independent of one another, it is possible to control the notch-frequency response so that it corresponds to two distinct notch bands. As a result, the metal strips change their electrical length, return loss, and radiation characteristics and are tested on a 36 mm × 30 mm RT-Duroid substrate that serves as a physical realisation of the intended antenna and serves to verify the accuracy of the simulation results.

2. PROPOSED ANTENNA GEOMETRY AND DESCRIPTION

The antenna is designed on a 36 mm×30 mm RT-Duroid substrate (relative permittivity = 2.2 and thickness = 0.762 mm). The ground plane size is 15 mm×30 mm and the feed-line size of 15.5 mm× 2 mm has been taken. The antenna consists of

Received : 25 February 2022, Revised : 12 March 2023
Accepted : 18 April 2023, Online published : 11 July 2023

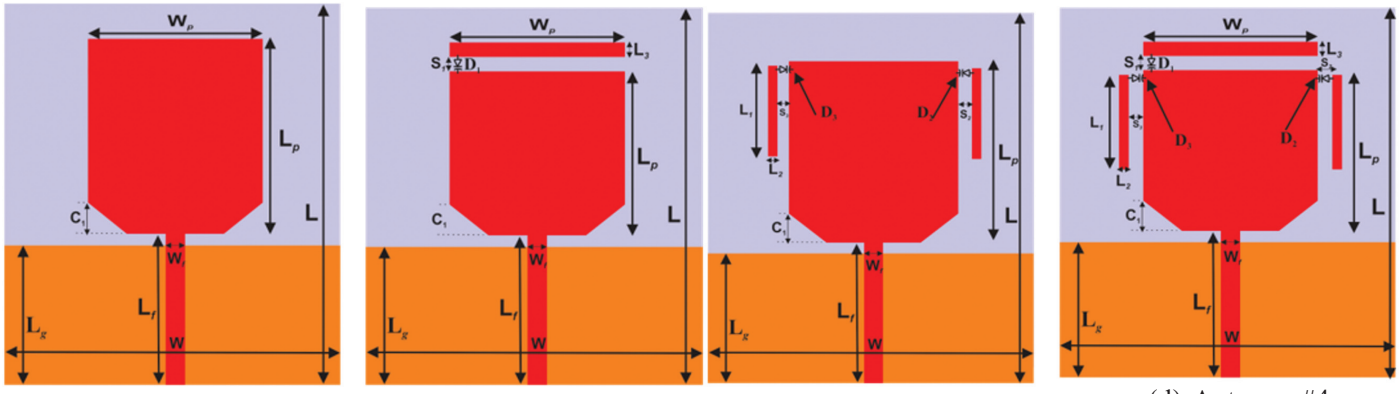

Figure 1. Geometry of the proposed tunable dual band-notched antenna for WiMAX/WLAN applications.

a radiating patch with three narrow conducting parasitic strips around the radiating patch. These strips are connected to the main radiating patch via three SMV 1405 varactor diodes. The purpose of using varactor diodes here is to produce dual-band notched tunable characteristics to avoid interference, including in IEEE 802.16 3.3 GHz WiMAX and IEEE 802.11a 5 GHz WLAN applications.

By adjusting the capacitance of three diodes with biasing, dual-notch behavior can be tuned within the UWB region. The capacitance associated with varactor D_1 between the horizontal strip and the radiating patch is C_1, whereas the capacitance associated with varactors D2 and D3 between I-shaped strips and the radiating patch is C_j. The varactor diode's capacitance values (C_1 and C_j) are optimised to be 2.2 pF and 2.2 pF. According to the datasheet of the SMV1405 diode, the series resistance and inductance values of the varactor are 0.85 Ω and 0.7 nH, respectively. Single-strand wires are attached to the anode and cathode terminals of the varactor and a DC supply voltage of 1.5 V is used to bias the varactor. Tunable band-notched characteristics are achieved independently by changing the capacitance value of the varactor from 0.63 pF to 2.63 pF, which corresponds to the biasing voltage from 30V-to-0V.

In Fig. 1, there are four antenna shapes, each of which is termed Antenna #1, Antenna #2, Antenna #3, and Antenna #4. As shown in Fig. 1, to create Antenna #2, place a thin horizontal strip on top of the reference patch geometry and use a varactor diode (D1) to connect one corner of the conducting strip to the patch's radiating edge. (b). Antenna #3 is formed by attaching two identically shaped, narrow parasitic strips to opposite sides, along the length of the reference radiating patch, as shown in Fig. 1(c). Again, Antenna #2 and Antenna #3 are merged to form Antenna #4. These are the optimised geometrical dimensions for these four antenna geometries: W = 30, L = 36, W_p = 18, L_p = 16, L_f = 15.5, W_f = 2, C_1 = 3 mm, L_g = 15, L_1 = 10, L_2 = 1, L_3 = 1.5, $S_1 = S_2 = S_3$ = 3. Here, all the dimensions are in mm. Here, L_p is the length and W_p is the width of the radiating patch. The 50 Ω microstrip feed line has a width of w_f and a length of l_f.

3. SIMULATED RESULTS AND DISCUSSION

The antenna is fabricated with an RT-Duroid substrate that is 0.762 mm thick and has a relative permittivity of 2.2.

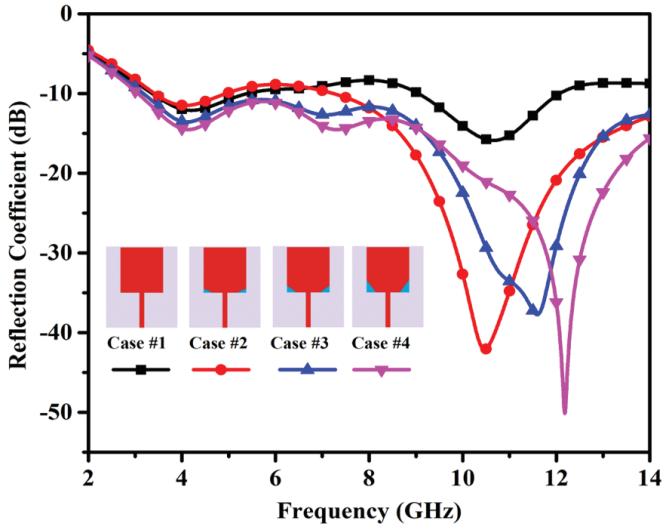

Figure 2. Simulated impedance matching variations in antenna #1.

In Section 2, the technique for designing Antenna #1, Antenna #2, Antenna #3, and Antenna #4 has been detailed, step-by-step. Antenna #1 is the reference UWB patch antenna that is designed for the following four different situations (Case #1, Case #2, Case #3, and Case #4): no truncation, truncation of 1mm (C1 = 1 mm), truncation of 2 mm (C1 = 2 mm), and truncation of 3mm (C1 = 3 mm). As shown in Fig. 2, the truncation is taken at an angle from the patch's bottom edge to its upper side. Consequently, a truncation of 3 mm (Case #4) produces a perfect impedance match within the ultra-wideband (UWB) range of up to 14 GHz.

For incorporating band-notch characteristics independently, the antenna layouts described in Fig. 1(a), are further modified, and these modified geometries (Antenna #2 and Antenna #3) are depicted in Fig. 1(b) and Fig. 1(c), respectively. Antenna #2 is analysed in three different cases, i.e. Case #1, Case #2, and Case #3. In Case #1, a narrow strip of width 'S_1' is removed from the top of the radiating patch. In Case #2, the upper copper strip is shorted to the main radiating patch with a copper thickness of 1.5 mm on the left corner, and finally, in Case #3, this 1.5mm copper strip is replaced by a varactor diode (D_1). Figure 3(a) shows how the reflection coefficient changes in these three situations. It is clear that there

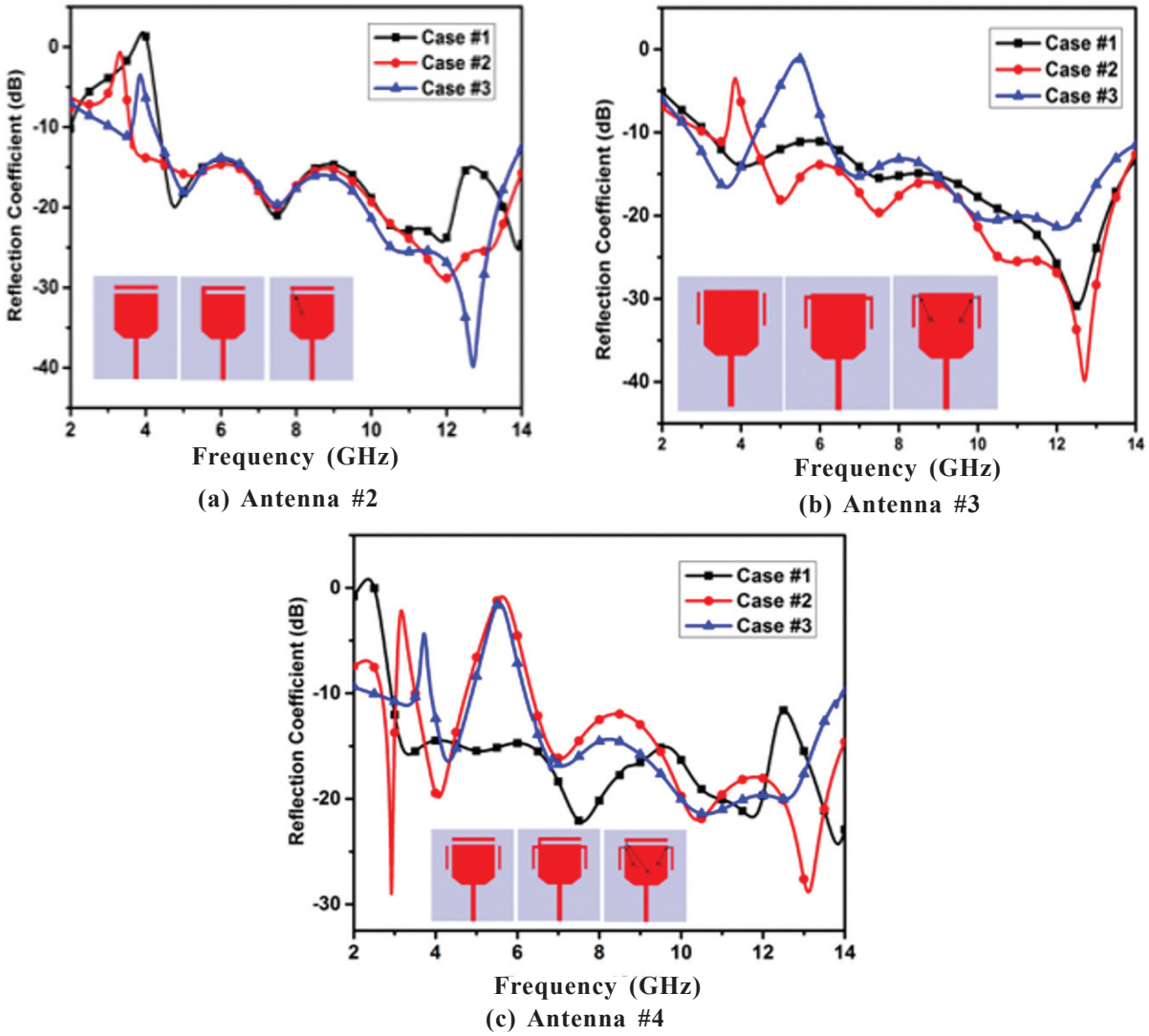

Figure 3. Simulated notch behaviors of three antennas.

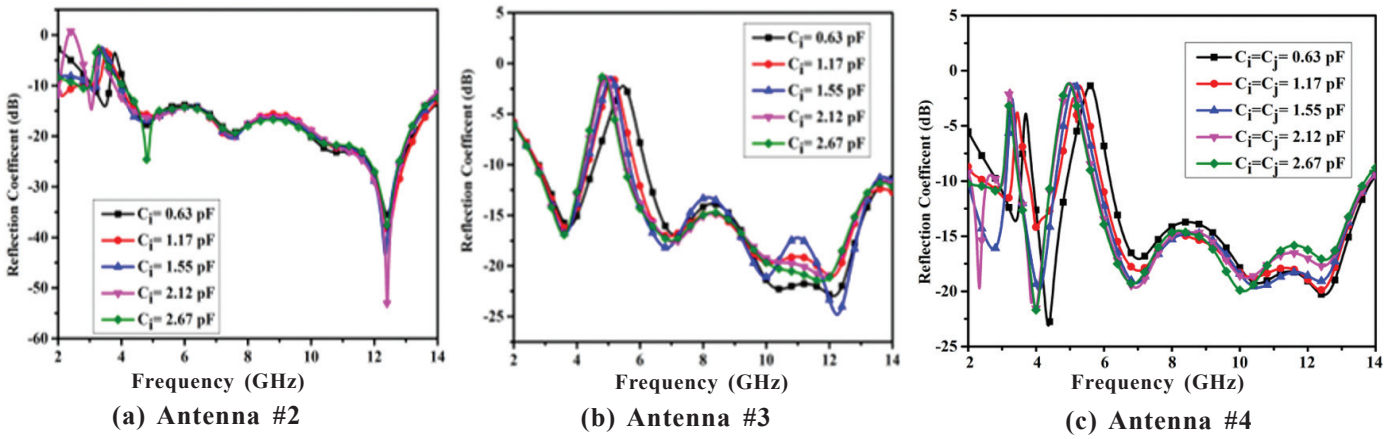

Figure 4. Tunability behaviours of three antenna geometries.

is a notch in all three cases, but only Case #3 has the notch at the desired frequency of 3.3 GHz.

The geometry of Antenna #3 is analysed by considering three distinct situations, namely Cases #1, #2, and #3. In Case #1, two narrow conducting parasitic strips are placed on the left and right sides of the primary radiating patch at a distance of 'S2'.

In Case #2, these two parasitic strips are shorted to the main radiating patch with a copper of 1.5 mm thickness, whereas in Case #3, out of these two copper thicknesses, each one is replaced by two varactor diodes (D_2 and D_3), respectively.

Table 1. Comparison of proposed work as compared to other similarly reported works in the literature

Ref.	Antenna size (mm^2)	Substrate (ε_r, thickness h)	Return loss BW	Peak gain	Notch bands	No. of notch band	Notch type	Type of switch
13	38.7×26.88	3, 0.1 mm	3.1-12 GHz	4	5.15-5.825	One	Reconfigurable	MEMS
14	36.6 × 26	4.3, 1.5 mm	2.5-9 GHz	NR	4.2–4.8 GHz or 5.8-6.5 GHz	One	Tunable & reconfigurable	PIN diode Varactor diode
15	100 × 100	3.2, 0.76 mm	3-11 GHz	2.2	4.5-5 GHz	One	Tunable	Varactor diode
16	42×30	3, 0.762 mm	3-12 GHz	4	4.77-6.21 GHz	One	Tunable	Varactor diode
17	40×40	2.2, 0.503 mm	2.8-11.9 GHz	4.2	4.4-5.4 GHz	One	Tunable	Varactor diode
18	40 × 20	4.4, 1 mm	3.18-11.26	5.41	3.31–3.99 GHz, 4.97–5.93 GHz	Two	Fixed	NA
[19]	40 × 40	3, 0.762 mm	2.8 - 11.34	~ 5	5.725–5.825 GHz 8.025–8.4 GHz	Two	Fixed	NA
[20]	40 × 32	4.4, 1.2 mm	3.04 to 11.4 GHz	~ 6.2	5.15-5.35 GHz 5.72-5.87 GHz	Two	Fixed	NA
[21]	31 × 18	4.4, 0.8 mm	3.07 – 12 GHz	~ 4	3.17–3.79, 5.14–6.82 GHz	Two	Reconfigurable	PIN
Proposed work	**36 × 30**	2.2, 0.762 mm	2-14 GHz	4.59	3.15-3.69 GHz, 4.93 GHz-5.59 GHz	Two	Tunable	Varactor

In these three cases of Antenna #3, the variations in the reflection coefficient are plotted in Fig. 3(b). It is clear here that a different notch is appearing in all three cases, but the notch at the desired frequency of 5 GHz is appearing only in Case #3. Now incorporating Antenna #2 and Antenna #3 geometries into a single one to form Antenna #4. This antenna geometry is also analysed by considering three cases, i.e., Case #1, Case #2, and Case #3. In Fig. 3(c), the variations in the reflection coefficient corresponding to each case are also plotted. It is observed here that in Antenna #4, two notches are appearing independently, one at 3.3 GHz and another at 5 GHz, respectively. For the introduction of the tuning behavior at two notch frequencies (i.e., 3.3 GHz and 5 GHz), the biasing of diodes D_1, D_2, and D_3 is varied between 0 V and 30 V (i.e., 2.67 pF and 0.63 pF) for Antenna #2, Antenna #3 and Antenna #4, respectively. Figures 4(a), 4(b), and 4(c) show the changes in the tunable reflection coefficient for these three antenna geometries. Antenna #2 can be tuned between 3.15 GHz and 3.69 GHz, while Antenna #3 can be tuned between 4.93 GHz and 5.59 GHz. In the case of Antenna #4, the tunability between 3.15 GHz and 3.69 GHz and between 4.93 GHz and 5.59 GHz is appearing simultaneously. Also, Table 1 shows how the proposed work compares to similar works that are already out there. The main contributions of the present work are:

- The design of a UWB antenna with tunable notches at dual frequencies. Similar works reported earlier (in Table 1) mainly focus on realizing single- or dual-band notches at fixed frequencies within the UWB operating range. But in many cases, it is necessary to tune these notch frequencies based on the application, which is the primary constraint in those works in[18-20] of Table 1
- Although few works have incorporated switching devices (MEMS, PIN, or varactor) to either reconfigure or tune the notch frequencies, at a single time their operation is limited to a single band notch frequency. While the present work in this paper proposes tuning the notch frequencies over dual bands (3.3 GHz WiMAX and 5 GHz WLAN)
- When the low dielectric constant of the substrate is taken into account, the proposed antenna is smaller than the other antennas in Table 1. The antenna exhibits a broader return loss BW of 12 GHz compared to other designs without any significant compromise with the gain and efficiency.

Figure 5 illustrates the surface current distribution of the proposed antenna at various frequencies to better clarify how the notched behavior works. Because of high attenuation, the surface current distribution is higher at horizontal (Fig. 5(a)) and vertical (Fig. 5(c)) stubs at dual-notch frequencies such as 3.5 GHz and 5.35 GHz. These current distributions of notched frequencies are plotted at 1.17 pF of a variable capacitance, which is equivalent to the varactor diode bias voltage of 5V. In addition, the surface current distribution at other frequencies such as 4.25 GHz (Fig. 5(b)) and 12.7 GHz (Fig. 5(d)) over a wide impedance band region is plotted to indicate that the strips have no effect on impedance matching other than at notch frequencies.

4. FABRICATION AND CHARACTERISATION

A prototype of the optimised Antenna #4 is fabricated and characterised for validation. Fig. 6 shows the prototype's top and bottom views. The antenna's reflection coefficient was measured using a vector network analyzer (VNA). A constant DC power supply supplies bias voltage for three varactors (D1, D2, and D3). For different bias voltages (like 0 V, 0.5 V, 2 V, 5 V, and 5 V) applied to both D_1 and D_2, simultaneously, the return

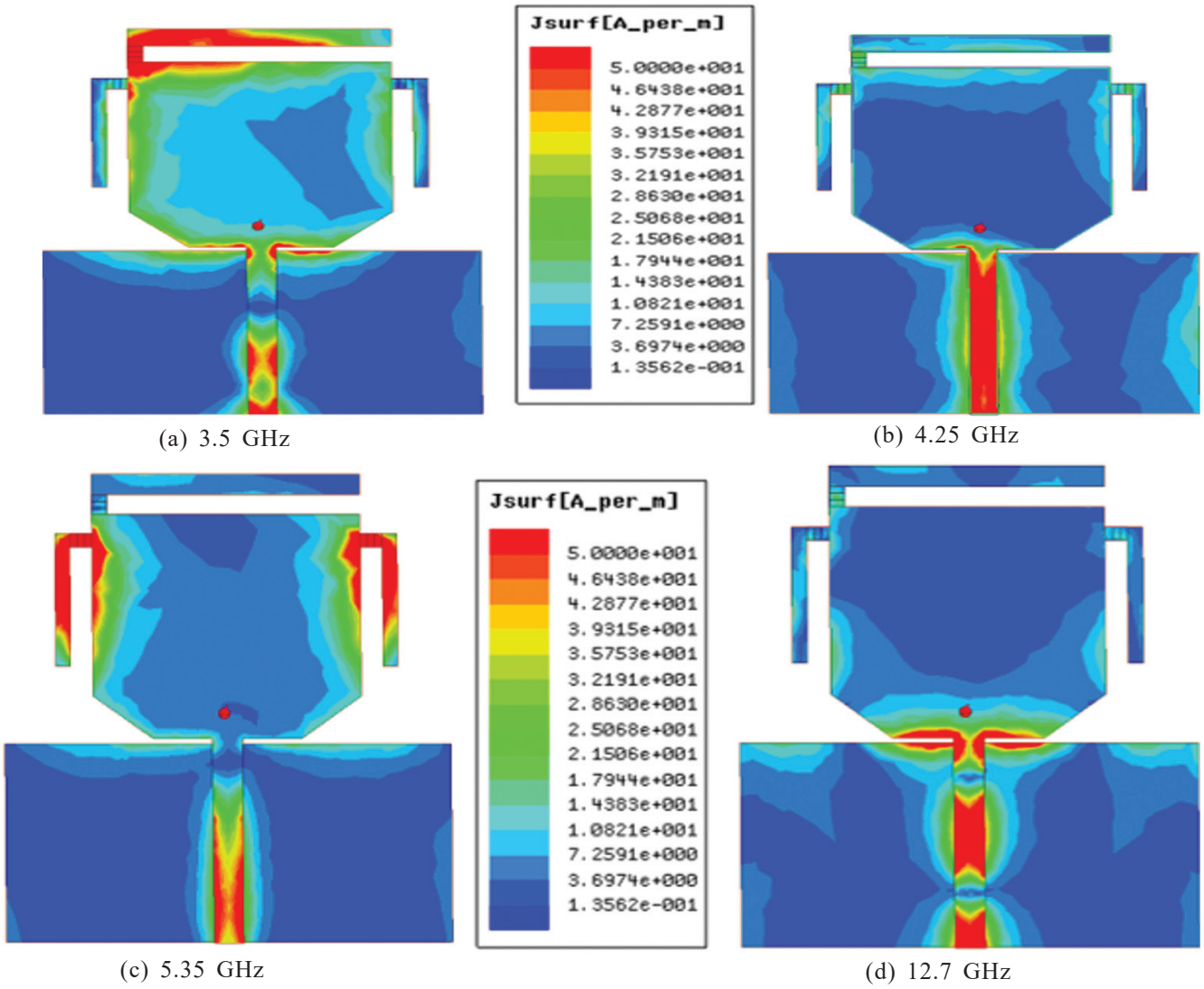

Figure 5. Surface current distributions on the antennas at different frequencies.

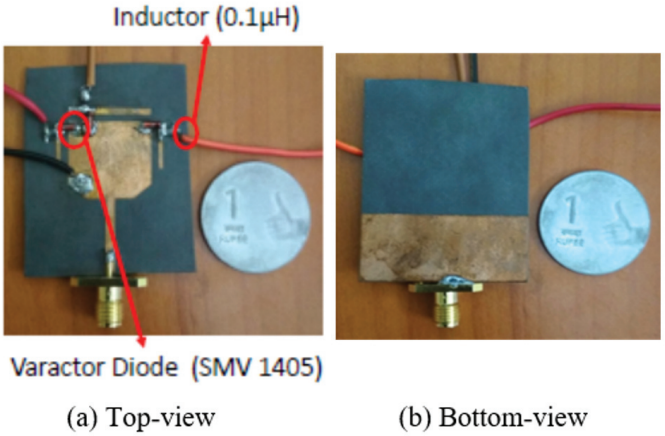

Figure 6. Fabricated prototype of the tunable notch antenna.

losses are measured. These coefficient values are measured using diode D1 biasing voltages of 0 V, 2 V, 5 V, and 30 V. Three different cases' simulated and measured performances are shown in Figure 4.7. Here $C_i = C_j = 2.67$ pF for Case #1, $C_i = C_j = 1.55$ pF for Case #2, and finally $C_i = C_j = 1.17$ pF for Case #3. The bias voltage corresponds to capacitances of 2.63, 1.55, and 1.17 pF at 0 V, 2 V, and 5 V respectively. Moreover, Ci relates to the capacitance of diode D1, while Cj refers to the capacitance of diodes D2 and D3, respectively. The simulated and measured return losses are compared in Fig. 7. Except for a small aberration, very good agreement is observed between simulated and measured results. Tolerances in fabrication and VNA calibration errors can cause this small disagreement. A good agreement is also observed between measured and simulated notch frequencies, as is clear from Table 2. Figure 4 illustrates measured and simulated radiation patterns in two principal planes, E and H, which are found to be closer. Figure 8 shows the simulated and measured gain and efficiency of the proposed UWB antenna with a 2 V bias voltage. At the two-notch frequencies, the gain and efficiency of the antenna decline significantly. The antenna's peak gain at 2 V is 4.59 dBi, and its efficiency is > 90 %. Note that 0 V and 5 V achieve negligible divergence (~ 0.3 dBi). As illustrated in Fig. 9, the radiation pattern of an antenna's far field in the E and H planes is simulated and measured. Similarities between simulated and measured radiation patterns are substantial.

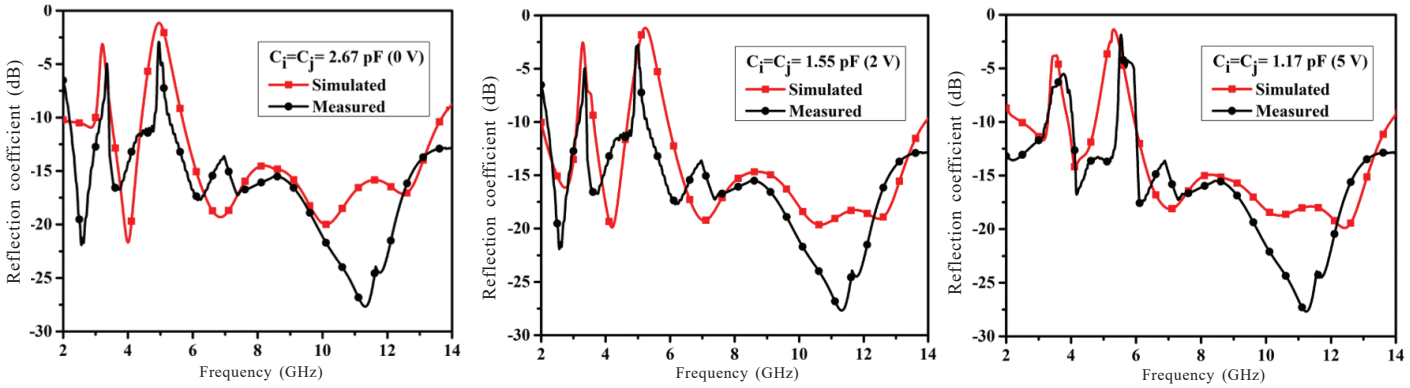

Figure 7. Simulated versus measured results comparison at three conditions, (a) Ci = Cj = 2.67 pF (0V), (b) Ci = Cj = 1.55 pF (2V), and (c) C_i = C_j = 1.17 pF (5V).

Table 2. Measured and simulated notch frequencies comparison

Case #1 (5V biasing)		Case #2 (2V biasing)		Case #3 (0V biasing)	
Measured values	**Simulated values**	**Measured values**	**Simulated values**	**Measured values**	**Simulated values**
3.70 GHz and 5.55 GHz	3.55 GHz and 5.4 GHz	3.35 GHz and 5.03 GHz	3.31 GHz and 5.15 GHz	3.30 GHz and 4.96 GHz	3.21 GHz and 4.90 GHz

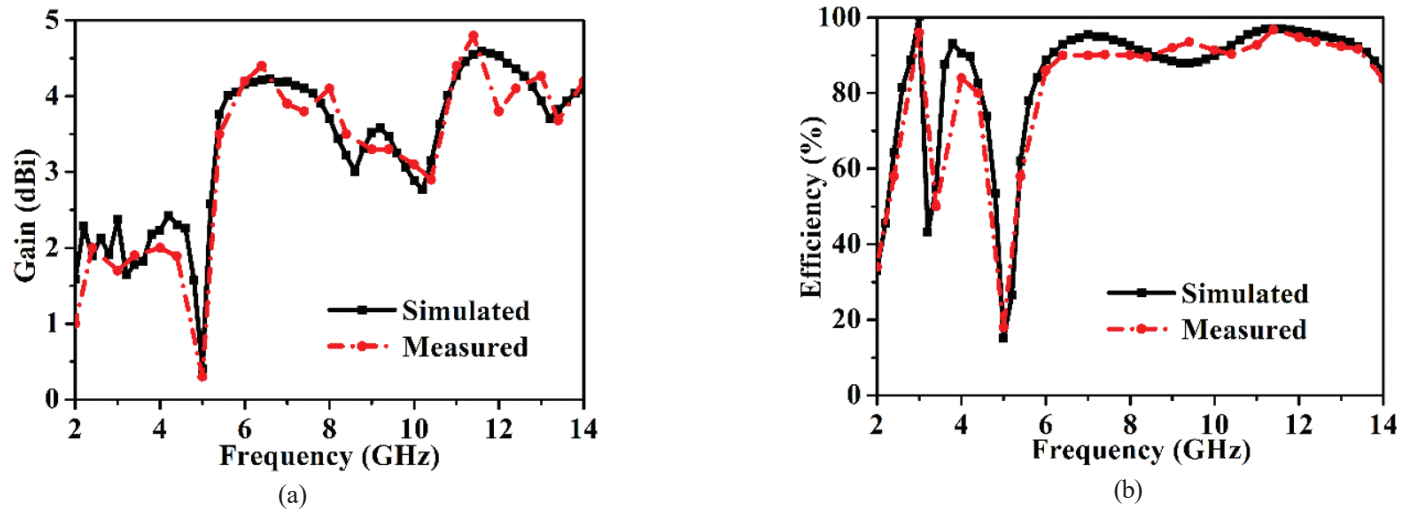

Figure 8. Simulated versus measured results comparison for (a) gain and (b) efficiency at Ci = Cj =1.55 pF (2 V).

5. CONCLUSIONS

A UWB band-notch antenna with dual frequency tuning has been presented. The WiMAX and WLAN band notch characteristics are independently regulated and continuously tunable by inserting a varactor diode in the radiating patch's upper right corner and a pair of diodes symmetrically on the patch's left and right sides. The results show that the antenna has attained an impedance bandwidth (S11<-10dB) from 2.6 GHz to 14 GHz, except for a tunable notch band between 3.15 GHz to 3.69 GHz and 4.93 GHz to 5.59 GHz by changing the electrical length using varactor diodes. The newly developed compact antenna radiates strongly in the E and H planes. The newly developed compact antenna radiates significantly in the E and H planes. The antenna has the potential application in future UWB systems.

REFERENCES

1. Federal Communications Commission: First Report and Order on Ultra-Wideband Technology, 2002, FCC **02**-48, Washington, DC.
2. Akbari, M.; Koohestani, M.; Ghobadi, Ch. & Nourinia, J. A new compact planar UWB monopole antenna. *Int. J. RF Microw. Comput., Aided Eng*., 2011, **21**(2), 216–220. doi: 10.1002/mmce.20507
3. Akbari, M.; Koohestani, M.; Ghobadi, Ch. & Nourinia, J. Compact CPW-Fed printed monopole antenna with super wideband performance, *Microw. Opt. Technol. Lett*., 2011, **53**(7), 1481-1483. doi: 10.1002/mop.26090
4. Mighani, M.; Akbari, M. & Felegari, N. Design of a small rhombic monopole antenna with parasitic rectangle into a slot of the feed line for SWB application, *Appl. Computat.*

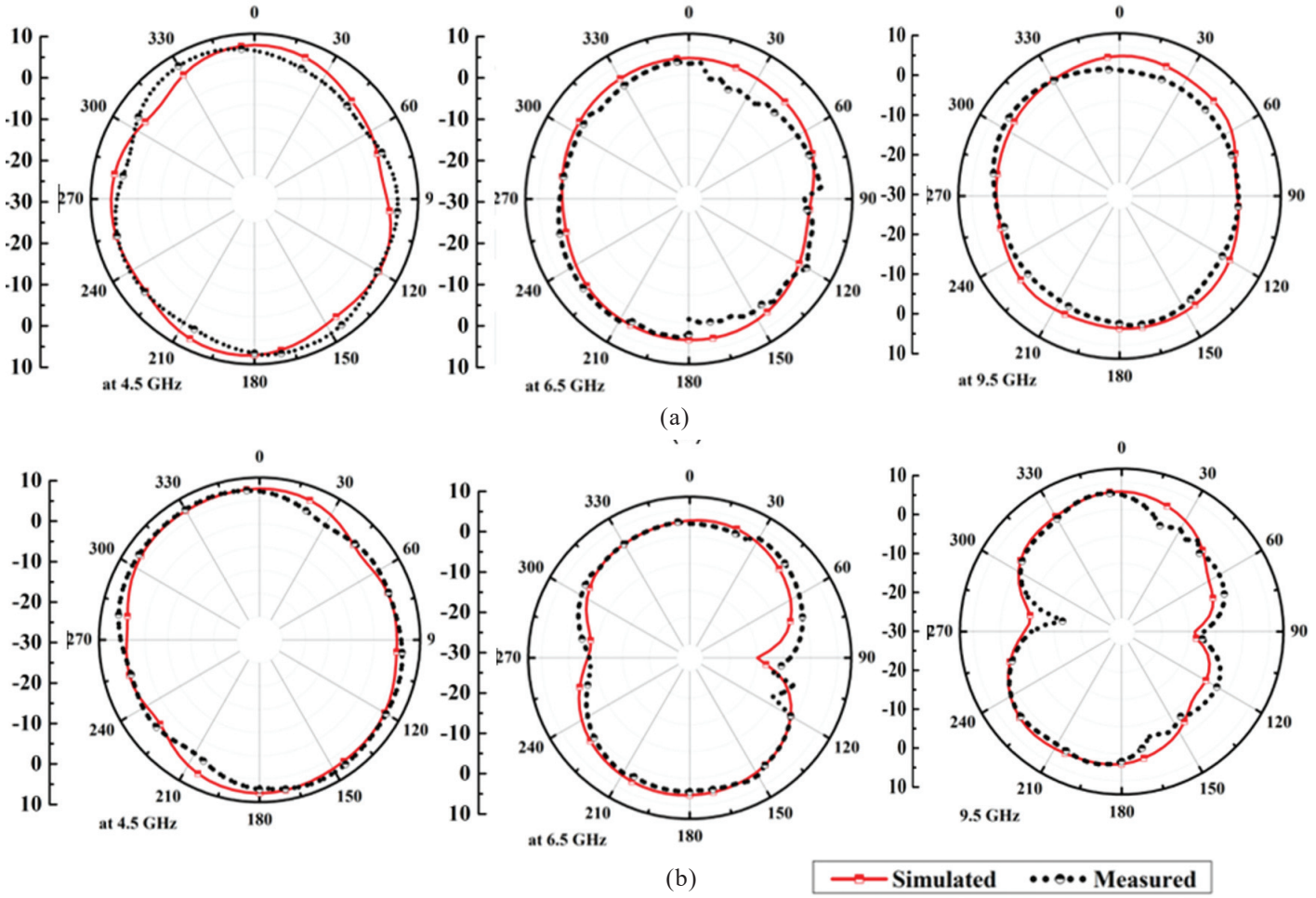

Figure 9. Simulated and measured radiation pattern: (a) H-plane, (b) E-plane at frequencies 4.5, 6.5, and 9.5 GHz.

Electromagn. Soc., 2012, **27**(1), 74-79.

5. Wong, K-L.; Chi, Y-W.; Su, C-M. & Chang, F-S. Band-notched ultra-wideband circular-disk monopole antenna with an arc-shaped slot, *Microw. Opt. Technol. Lett.*, 2005, **45**(3), 88-191. doi: 10.1002/mop.20766
6. Cho, Y.J.; Kim, K.H.; Choi, D. H.; Lee, S.S. & Park, S.O. A miniature UWB planar monopole antenna with 5 GHz band rejection filter and the time domain characteristics, *IEEE Trans. Antennas Propag.,* 2006, **54**(5), 1453-1460. doi: 10.1109/TAP.2006.874354
7. Chu, Q.X. & Yang, Y.Y. A compact ultra-wideband antenna with 3.4/5.5 GHz dual band-notched characteristics, *IEEE Trans. Antennas Propag.*, 2008, **56**(12), 3637–3644. doi: 10.1109/TAP.2008.2007368
8. Peng, L.; Ruan, C.L. & Yin, X.C. Analysis of the small slot-loaded elliptical-patch antenna with a band-notched for UWB applications, *Microw. Opt. Technol. Lett.*, 2009, **51**(4), 973–976. doi: 10.1002/mop.24247
9. Dong, Y.D.; Hong, W.; Kuai, Z.Q. & Chen, J.X. Analysis of planar ultrawide-band antennas with on-ground slot band-notched structures, *IEEE Trans. Antennas Propag.*, 2009, **57**(7), 1886–1893. doi: 10.1109/TAP.2009.2021910
10. Kim, K.H. & Park, S.O. Analysis of the small band-rejected antenna with the parasitic strip for UWB, *IEEE Trans. Antennas Propag.*, 2006, **54**(6), 1688–1692. doi: 10.1109/TAP.2006.875911
11. Abbosh, A.M. & Bialkowski, M.E. Design of UWB planar band-notched antenna using parasitic elements, *IEEE Trans. Antennas Propag.*, 2009, **57**(3), 796–799. doi: 10.1109/TAP.2009.2013449
12. Peng, L.; Ruan, C.L.; Chen, Y.L. & Zhang, G.M. A novel band notched elliptical ring monopole antenna with a coplanar parasitic elliptical-patch for UWB applications, *J. Electromagn. Waves Appl*., 2008, **22**(4), 517–528.
13. Nikolaou, S.; Kingsley, N.D.; Ponchak, G.E.; Papapolymerou, J. & Tentzeris, M.M. UWB elliptical monopoles with a reconfigurable band notch using MEMS switches actuated without bias lines, *IEEE Trans. Antennas Propag*., 2009, **57**(8), 2242–2251. doi: 10.1109/TAP.2009.2024450
14. Wei, W.; Yun-Bo, L.; Rui, Y.W.; Chuan-Bo, S. & Tie-Jun, C. Band-Notched UWB antenna with switchable and tunable performance. *Int. J. Antennas Propag.*, 2016, **2016**(1), 1-6. doi: 10.1155/2016/9612987
15. Antonino Daviu, E.; Cabedo Fabres, M.; Ferrando-Bataller, M. & Vila Jamenez, A. Active UWB antenna

with tunable band-notched behavior, *Electron. Lett*., 2007, **43**(18), 959–960.
doi: 10.1049/el:20071567

16. Atallah, H.A.; Adel, B.; Abdel-Rahman, Yoshitomi, K. & Pokharel, R.K. Tunable band-notched CPW-Fed UWB monopole antenna using capacitively loaded microstrip resonator for cognitive radio applications, *Progress Electromagn. Res.* C., 2016, **62**(1), 109–117.
doi: 10.2528/pierc16010501
17. Hua, C.; Lu., Y. & Liu, T. UWB heart-shaped planar monopole antenna with a reconfigurable notched band, *Progress Electromagn. Res. Lett.*, 2017, **65**(1), 123–130.
doi: 10.2528/PIERL16120203.
18. Devana, V.N.R. & Rao, A.M. A novel dual band-notched mimo uwb antenna. *Progress Electromagn. Lett*., 2020, **93**, 65–71.
19. Atallah, H.A.; Abdel-Rahman, A.B.; Yoshitomi, K. & Pokharel, R.K. Design of dual band-notched cpw-fed UWB planar monopole antenna using microstrip resonators. *Progress Electromagn. Lett.*, 2016, **59**, 51–56.
20. Ding, T.; Wang, M.; Guo, J.; Zhang, L. & Xiao, J. A wrench-shaped uwb antenna yielding dual notched bands for WLAN application. *Appl. Comput. Electromagn. Soc. J. (ACES)*, 2022, 297–304.
21. Han, L.; Chen, J. & Zhang,W. Compact uwb monopole antenna with reconfigurable band-notch characteristics. *Int. J. Microwave Wireless Technol.*, 2020, **12**(3), 252–258.
22. Safia, O. Abu.; Nedil, Mourad.; Talbi, L. & Hettak, K. Coplanar waveguide-fed rose-curve shape UWB monopole antenna with dual-notch characteristics, *IET Microwaves, Antennas & Propagation*, 2018, **12**(7), 1112 – 1119.
doi: 10.1049/iet-map.2017.0852
23. Zhao, X.; Yeo, S.P. & Ong., L.C. Planar UWB MIMO antenna with pattern diversity and isolation improvement for mobile platform based on the theory of characteristic modes, *IEEE Trans. Antennas Propag*., 2018, **66**(1), 420–425.
doi: 10.1109/TAP.2017.2768083
24. Li, D.H.; Zhang, F.S.; Cao, L.X. & Zhao, Y. A compact dual band-rejected MIMO Vivaldi antenna for UWB wireless applications. *Progress Electromagn. Res. Lett.*, 2019, **86**(1), 97-105.
doi: 10.2528/PIERL19062506
25. Rahman, M.; Haider, A. & Naghshvarianjahromi, M. A systematic methodology for the time-domain ringing reduction in UWB band-notched antennas, *IEEE Antennas Wireless Propag. Lett.*, 2020, **19**(3), 482-486.
doi: 10.1109/LAWP.2020.2972025
26. Chen, Z.; Zhou, W. & Hong, J. A miniaturised MIMO antenna with triple band-notched characteristics for UWB applications, *IEEE Access*., 2021, **9**(1), 63646 - 63655.
doi: 10.1109/ACCESS.2021.3074511
27. Elsharkawy, R.R.; Abd El-Hameed, A.S. & El-Nady, S.M. Quad-port MIMO filtenna with high isolation employing BPF with high out-of-band rejection, *IEEE Access*., 2022, **10**(1), 3814 - 3824.
doi: 10.1109/ACCESS.2021.3134865

CONTRIBUTORS

Mr Vikas Kumar Rai obtained his PhD degree in RF Communication Engineering from the Rajasthan Technical University, Kota, Rajasthan. His current research interests include RF Communication, UWB Active Antenna, Microstrip Antenna, Microwave Device Designing Technology, and MOS technology.
In the present work, he developed the design and prepared the initial draft of the manuscript.

Dr Mithilesh Kumar obtained his PhD degree in RF Communication Engineering from the IIT, Delhi. India. His current research interests include RF Communication, UWB Active Antenna, Microstrip Antenna, and Microwave Device Designing Technology.
In the present work, he provided the conceptual framework and supervised the work.